

EXPANSION AND BRIGHTNESS CHANGES IN THE PULSAR-WIND NEBULA IN THE COMPOSITE SUPERNOVA REMNANT KES 75

STEPHEN P. REYNOLDS,¹ KAZIMIERZ J. BORKOWSKI,¹ AND PETER H. GWYNNE¹

¹*Department of Physics, North Carolina State University, Raleigh, NC 27695-8202, USA*

ABSTRACT

We report new *Chandra* X-ray observations of the shell supernova remnant (SNR) Kes 75 (G29.7–0.3) containing a pulsar and pulsar-wind nebula (PWN). Expansion of the PWN is apparent across the four epochs, 2000, 2006, 2009, and 2016. We find an expansion rate between 2000 and 2016 of the NW edge of the PWN of $0.249\% \pm 0.023\% \text{ yr}^{-1}$, for an expansion age $R/(dR/dt)$ of 400 ± 40 years and an expansion velocity of about 1000 km s^{-1} . We suggest that the PWN is expanding into an asymmetric nickel bubble in a conventional Type IIP supernova. Some acceleration of the PWN expansion is likely, giving a true age of 480 ± 50 years. The pulsar’s birth luminosity was larger than the current value by a factor of 3–8, while the initial period was within a factor of 2 of its current value. We confirm directly that Kes 75 contains the youngest known PWN, and hence youngest known pulsar. The pulsar PSR J1846–0258 has a spindown-inferred magnetic field of $5 \times 10^{13} \text{ G}$; in 2006 it emitted five magnetar-like short X-ray bursts, but its spindown luminosity has not changed significantly. However, the flux of the PWN has decreased by about 10% between 2009 and 2016, almost entirely in the northern half. A bright knot has declined by 30% since 2006. During this time, the photon indices of the power-law models did not change. This flux change is too rapid to be due to normal PWN evolution in one-zone models.

Keywords: ISM: individual objects (Kes 75) — ISM: supernova remnants — X-rays: ISM

arXiv:1803.09128v1 [astro-ph.HE] 24 Mar 2018

1. INTRODUCTION

Pulsar-wind nebulae (PWNe) provide essential information on various astrophysical phenomena. As pulsar calorimeters, they document the total energy injected by the pulsars, independent of beaming. The relativistic-wind termination shocks through which energetic particles enter the PWNe can serve as nearby laboratories in which to study particle acceleration in relativistic winds and jets such as those seen in active galactic nuclei and gamma-ray burst sources. Young PWNe, still inside their natal shell supernova remnant (SNR), interact with the innermost ejecta and can provide information about that material, otherwise inaccessible. The youngest PWNe also give information on the youngest pulsars, whose behavior may differ from that of the more typical pulsars that have long outlasted or escaped from their SNRs.

While most supernovae (SNe) should result from core-collapse (CC) events, and almost all CCSNe need to produce pulsars to produce the present-day Galactic pulsar population (Lorimer et al. 2006), it is a bit surprising that of four confirmed historical SNRs (Kepler 1604 CE, Tycho 1572, Crab 1054, and SN 1006) and two more expansion-confirmed SNRs (G1.9+0.3, ca. 1900, and Cas A, ca. 1680), none is a composite remnant (shell + PWN). (3C 58 is a Crab-like PWN with no obvious shell, and in any case is unlikely to be the remnant of an event in 1181 CE; e.g., Chevalier 2005). Now young pulsars can manifest themselves through short spindown ages $P/(n-1)\dot{P}$, which are upper limits to the true ages under the assumption of normal dipole spindown with constant braking index n . One such object, G11.2-0.3, a shell remnant containing an observed pulsar and PWN, was recently found to have an age between 1400 and 2400 years, based on observations with *Chandra* between 2000 and 2013, though it cannot have resulted from a possible supernova in 386 CE (Borkowski et al. 2016). This age is much less than its spindown age of about 23,000 years, which must be far larger than the true age based on several arguments including the pulsar position at the very center (Kaspi et al. 2001), and requiring that the pulsar period be essentially unchanged from birth.

One other composite remnant might conceivably have resulted from a supernova in the last two millennia: Kes 75 (G29.7-0.3) (Becker & Kundu 1976; Becker et al. 1983, see Figure 1). An earlier distance estimate of 19 kpc made Kes 75 a very large, luminous object, but subsequent H I observations (Leahy & Tian 2008) gave a distance of 5.5 – 5.9 kpc. We shall adopt a value of 5.8 ± 0.5 kpc based on the reanalysis of Verbiest et al. (2012). At that distance, $1'' = 8.7 \times 10^{16}$ cm. The remnant shows a partial shell of radius about $90''$, or about 2.5 pc, with a central nebula of distinct properties, about $25'' \times 35''$ in extent (0.70×0.99 pc). The complete absence of detectable shell emission to the east indicates a very strong density gradient in the medium into which Kes 75 is expanding.

The central component was shown to have a flat radio spectrum with substantial polarization: a typical radio PWN (Becker & Kundu 1976). It was presumed to be powered by a

pulsar, but the pulsar was not discovered until 2000, in X-rays with *RXTE* (Gotthelf et al. 2000). (It still has not been detected in radio; Archibald et al. 2008). At that time, the pulsar, PSR J1846-0258, was found to have a period P of 326 ms, a remarkably high spindown luminosity of 8×10^{36} erg s^{-1} , and a high magnetic field (for a rotation-powered pulsar) of about 5×10^{13} G. This magnetic-field strength is within the range of the so-called magnetars, neutron stars with $B \gtrsim 10^{13.5}$ G powered by magnetic-field decay. The pulsar braking index was found by Livingstone et al. (2006) to be $n = 2.65 \pm 0.01$, which gave a spindown age $P/(n-1)\dot{P}$ of 884 years, the smallest known, and implying that Kes 75 is one of the youngest supernova remnants in the Galaxy. Kes 75 has also been detected between 20 and 200 keV with INTEGRAL (McBride et al. 2008) and between 0.3 and 5 TeV with HESS (Terrier et al. 2008), though neither instrument can distinguish between emission from the shell and from the PWN.

The pulsar in Kes 75 has proved to be highly unusual in several respects beyond its high magnetic field. In 2006 (just seven days before a long *Chandra* observation), the pulsar emitted a series of five magnetar-like short X-ray bursts (Gavriil et al. 2008), with a concomitant increase in the pulsar luminosity by about a factor of 6, along with spectral softening (Ng et al. 2008). It was later shown that the spindown properties of the pulsar had changed: evidently a glitch occurred sometime between 2005 (when the dataset fixing the earlier braking index ended) and 2008, when a new set of phase-coherent observations began (Archibald et al. 2015). Presumably the glitch was coincident with the X-ray bursts, though the observations do not demand this. The braking index was found to have decreased to 2.19 ± 0.03 , determined over a 7-year period. The new spindown age is now 1230 years, still among the shortest known. However, it is important to note that the pulsar’s spindown luminosity has not changed significantly from its pre-flare value. A change in n of this size, for one of the few pulsars for which timing data allow a determination of the second period derivative, is unprecedented.

Comparison of observations of the PWN with *Chandra* in 2000 and 2006 showed significant changes in the small-scale structure of the PWN, with apparent motion of one feature giving a speed of $0.03c$ (Ng et al. 2008). A jet-torus structure was identified, as often seen in young PWNe. Ng et al. (2008) performed detailed spatial analysis of the Kes 75 PWN, fitting individual spectra to 14 separate regions, and carefully comparing the 2006 observation to that from 2000. They found typical spectral behavior: a fairly hard spectrum (photon index $\Gamma = 1.9$ where $F_\nu \propto E^{-\Gamma}$) near the pulsar, with the spectrum softening with distance from the pulsar, although the very hardest spectrum ($\Gamma = 1.5$) was found not in the immediate neighborhood of the pulsar but a few arcsec away. They found no significant changes in Γ for the subregions between 2000 and 2006. Another observation (Livingstone et al. 2011) was performed in 2009 using 1/8 subarray mode, allowing a readout time of only 0.4 s to ameliorate pileup (but as a result, mostly restricted to the pul-

sar/PWN region). These authors reported an integrated flux of the PWN between 0.5 and 10 keV consistent with that from 2000, in spite of the remarkable pulsar outbursts and longer-term change in properties in 2006.

Several theoretical models for the evolution of Kes 75 have appeared recently, aiming to explain the full radio-to-TeV spectral energy distribution. [Bucciantini et al. \(2011\)](#) describe an evolutionary one-zone model, for which the data are quite constraining. They require an additional seed photon field to account for the TeV emission, and a very high efficiency of injection of particles. They infer a current mean magnetic-field strength of 20 – 30 μG . [Gelfand et al. \(2014\)](#) describe a similar model, based on the pre-flare pulsar properties, and infer an age of about 420 years. One justification for such simple models in the face of obvious highly complex and inhomogeneous observed PWNe has been that the relativistic sound speed in a PWN, $c/\sqrt{3}$, is so high that the pulsar bubbles should be essentially isobaric. Overall, one-zone (“zero-dimensional”) models do a surprisingly effective job of describing the broadband spectral-energy distribution of PWNe.

One-zone models also predict the gradual evolution of PWN properties. PWNe are expected to evolve in luminosity as they expand. The timescale for such evolution, due to adiabatic expansion losses and the slow decline of pulsar input power, is normally the dynamical timescale, comparable to the PWN age. Radiative properties can change on the timescale of energy losses on particles, much longer than the dynamical time for radio-emitting particles but only a few years for X-ray-synchrotron-emitting electrons and positrons in typical magnetic fields of tens to hundreds of μG . Simple evolutionary models (e.g., [Reynolds & Chevalier 1984](#); [Gelfand et al. 2009](#); [Bucciantini et al. 2011](#)) make quantitative predictions (explicitly or implicitly) for the time-dependence of the luminosity in different wavelength regimes, but these predictions have rarely been tested. One exception is the radio flux of the Crab Nebula, predicted by [Reynolds & Chevalier \(1984, hereafter RC84\)](#) to be declining at radio wavelengths at $(0.26 \pm 0.1)\% \text{ yr}^{-1}$, a prediction verified by [Aller & Reynolds \(1985\)](#). These are global predictions for integrated fluxes, and expected rates of change are slow. Small-scale brightness changes, on the other hand, have been followed in a few well-known cases, including the Crab wisps and X-ray knot ([Hester 2008](#)) and the Vela jet ([Durant et al. 2013](#)), and several other PWNe including Kes 75 show motions of small features ([Ng et al. 2008](#)).

One-zone models also assume the applicability of the simplest dipole-spindown models for pulsars. For normal magnetic-dipole spindown with constant n , the spindown age $t_{\text{sd}} \equiv P/(n-1)\dot{P}$ increases with time: $t_{\text{sd}} = \tau + t$ where $\tau \equiv t_{\text{sd}}(0)$ is the spindown time at birth. Then the pulsar luminosity $L(t)$ decays as

$$L(t) = \frac{L_0}{(1 + t/\tau)^p} \quad \text{where } p \equiv \frac{n+1}{n-1}. \quad (1)$$

The pulsar period P then obeys $P = P_0 (L_0/L)^{1/n+1}$. However, for pure magnetic-dipole field configurations, the brak-

Table 1. *Chandra* Observations of Kes 75

Date	Observation ID	Roll Angle (deg)	Effective Expo- sure Time (ks)
2000 Oct 15–16	748	279	31.68
2006 Jun 05	7337	133	17.36
2006 Jun 07–08	6686	133	49.02
2006 Jun 09	7338	133	39.25
2006 Jun 12–13	7339	133	44.05
2009 Aug 10–11	10938	249	44.25
2016 Jun 08–09	18030	133	84.76
2016 Jun 11–12	18866	133	60.99

ing index $n = 3$, which is never observed among the dozen or so pulsars with measured braking indices ([Espinoza et al. 2017](#)). More complex field geometries, and other modifications of the simple picture, have been proposed to account for observed values of n (e.g., [Gao et al. 2017](#); [Akgün et al. 2017](#); [Antonopoulou et al. 2018](#)); these models produce different spindown histories than simple dipole spindown.

For Kes 75, the significant changes in pulsar spindown properties observed since 2006 cast an additional shadow of uncertainty over the age estimates based on simple dipole spindown. But if Kes 75 is really less than 1000 years old, and at a distance of only about 6 kpc, its expansion should be measurable. On this basis, we obtained a 150 ks *Chandra* exposure in 2016.

2. OBSERVATIONS

Chandra observed Kes 75 at three epochs during its first decade of operations: in 2000 (Epoch I), 2006 (Epoch II), and 2009 (Epoch III). The most recent Epoch IV observation with *Chandra* took place in 2016 June in two separate pointings (Table 1), with the remnant again placed on the Advanced CCD Imaging Spectrometer (ACIS) S3 chip. Very Faint mode was used in order to reduce the particle background for this low surface brightness target. We used CIAO version 4.9 and CALDB version 4.7.4 to reprocess these Epoch IV observations. The bright central pulsar J1846–0258 was used to align the 2016 June 08–09 and 11–12 observations. After screening for particle flares, the total effective exposure time is 146 ks.

Epoch I–III observations (Table 1) were reprocessed as for Epoch IV, but the particle background rate is higher at Epochs I and III because Faint mode was used instead of Very Faint mode for these relatively shallow (32 and 44 ks) observations. For Epoch II, the total effective exposure is 150 ks,

comparable in length to Epoch IV. Three shorter pointings from 2006 (observation IDs 7337 – 7339) were aligned to the longest 2006 pointing (observation ID 6686).

The pulsar J1846–0258 was used for the inter-epoch alignment. It is by far the brightest point source in the *Chandra* field of view, located close ($< 1'.1$) to the optical axis, so its position can be determined with high precision for each observation listed in Table 1. In order to measure its position, we applied the CIAO task `srcextent` to data processed with Faint (instead of Very Faint) mode as appropriate for bright point sources. The pulsar’s point spread function (PSF) is approximated by a 2D Gaussian in `srcextent`, allowing us to find its centroid and width after fitting this Gaussian to the data. The estimated¹ positional uncertainties do not exceed 22 mas (at 90% confidence level). This corresponds to 1σ relative errors of $< 0.1\%$ at a radial distance of $15''$ away from the pulsar. As this is much smaller than the statistical errors of our expansion measurements, alignment errors relative to the pulsar’s reference frame can be safely ignored.

Although the pulsar’s reference frame is most appropriate for measuring the expansion of the PWN, there is a possibility of a substantial (several hundred km s^{-1}) pulsar kick. In the framework of freely expanding uniform ejecta discussed in § 5, this would have resulted in a nonnegligible net motion of the entire PWN/PSR system relative to the SN and its local frame of reference, but otherwise without any influence on the PWN dynamics. If large enough, the tangential component of this motion would manifest itself as a measurable proper motion of the pulsar relative to background and foreground point sources. Then, these sources would appear misaligned in the pulsar’s reference frame, particularly between Epochs I and IV.

We examined the relative positions of sufficiently bright point sources between Epochs I and IV (after alignment of observations to the pulsar reference frame). The relatively short (32 ks) duration of the Epoch I observation limits the number of matching sources suitable for reasonably accurate measurements to 10. They are rather faint on average, with a median number of counts of only 19 at Epoch I. Their off-axis angles range from $1'.2$ to $3'.8$. Their positions were found using the CIAO task `wavdetect`, while 1σ positional errors were estimated using equation (14) of Kim et al. (2007). These positions differ by an average of $\Delta\alpha \cos\delta = -120$ mas and $\Delta\delta = -30$ mas between Epochs I and IV, but there is a large scatter (210 mas and 170 mas, respectively) around these values. The measured point source displacements range from 95 to 680 mas, with the median of 160 mas. After their normalization by 1σ errors, they range from 0.27 to 2.2. Their distribution is well described by the Rayleigh distribution with a scale of 0.83 ± 0.13 (estimated using the method of maximum likelihood) that is statistically consistent with unity. Therefore, we find no evidence for misalignment of

¹ See equation (11) in Houck, J. C. 2007, http://cxc.harvard.edu/csc/memos/files/Houck_source_extent.pdf.

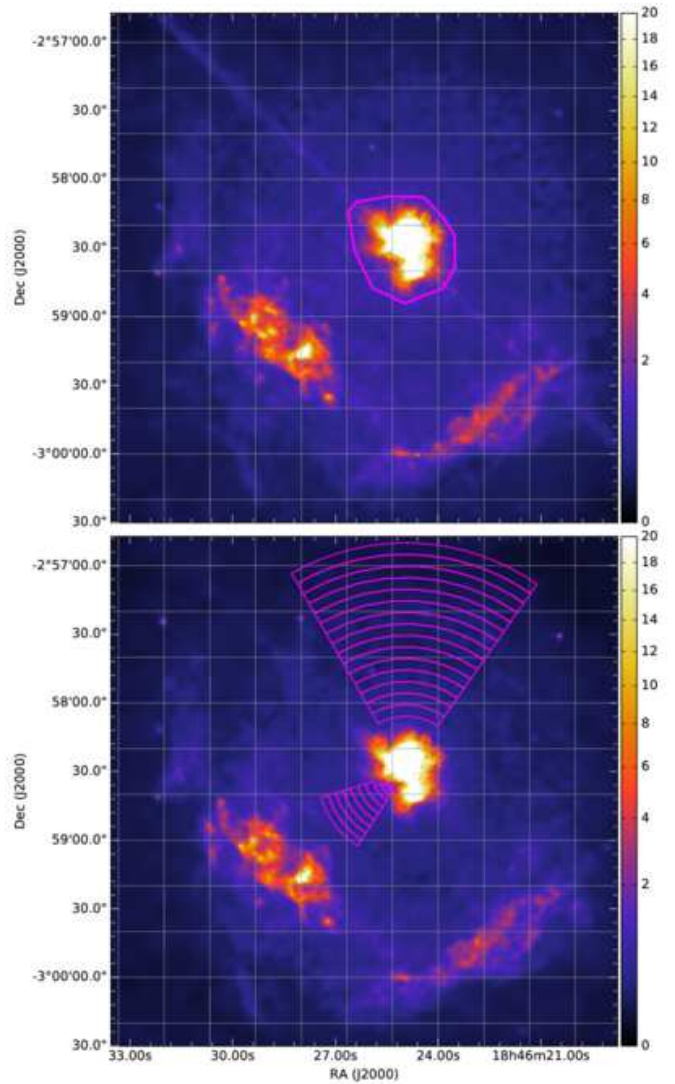


Figure 1. X-ray images of Kes 75 in the 0.7–8 keV energy range from 2006 (top) and 2016 (bottom), smoothed with the multiscale partitioning method of Krishnamurthy et al. (2010). The bright pulsar wind nebula at its center is saturated in order to show the much fainter shell structure. The 2006 image also shows the region used for flux extraction of the entire PWN. A dust-scattered halo is apparent in 2006. Its radial profile (see Figure 2) was measured within overlaid regions on the 2016 image. The scales are in counts per $0'.432 \times 0'.432$ image pixel.

point sources or a discernible pulsar motion. This conclusion must be considered as tentative because our `wavdetect`-derived positions do not rely on realistic models of the *Chandra* PSF.

Epoch II and IV images of Kes 75, extracted from merged and smoothed *Chandra* data cubes, are shown in Figure 1. Expansion of the shell is subtle but discernible by eye with the help of the coordinate grid, and its complex motion will be described in a separate investigation. Out-of-time events from the pulsar can be seen as diagonal “streaks” in these

images, being much more prominent in 2006 because of the much brighter pulsar at this epoch. Excess emission in the interior of the remnant is also apparent at this epoch, presumably a halo produced by scattering of the pulsar’s X-rays by interstellar dust present along the line of sight to Kes 75. This excess emission had been noticed previously (Ng et al. 2008), but now we can examine it in more detail by comparing the images shown in Figure 1. This contaminating halo emission must be taken into account when measuring expansion of the PWN.

The XSPEC spectral analysis package (Arnaud 1996) was used to examine X-ray spectra, which were extracted from individual observations and added together to obtain merged spectra. (The response files for each epoch’s obsID’s were averaged). Spectra of Kes 75 PWN were modeled with an absorbed power law, using the solar abundances of Grevesse & Sauval (1998) in the `phabs` absorption model. In order to preserve the Poisson nature of the statistics, we modeled rather than subtracted background for spectral fitting.

3. EXPANSION OF THE PWN

The time baselines between Epochs I – III and Epoch IV range from 6.83 to 15.65 years, long enough to reliably measure expansion of the PWN. We use a variation of the method described by us previously in our studies of the youngest Galactic SNR G1.9+0.3 (Carlton et al. 2011; Borkowski et al. 2014) and young CC SNRs G11.2–0.3 and Kes 73 (Borkowski et al. 2016; Borkowski & Reynolds 2017). First, we extracted two data cubes from the merged Epoch II and the merged Epoch IV observations, with 300^2 image pixels and 16 spectral channels, in the energy range from 0.7 to 8 keV, encompassing the entire PWN. The spatial pixel size is $0''.216 \times 0''.216$. We then removed the bright pulsar from these data cubes by masking it with a circle $2''.4$ in diameter. In each spectral channel, we replaced pixel values within this circle by simulated values assuming that the mean surface brightness there is constant and equal to the mean surface brightness within an ellipse centered on the pulsar, $5''.4 \times 2''.7$ in size and with its long axis perpendicular to the PWN jet. Poisson statistics were assumed in these simulations. We rebinned these filtered data cubes by a factor of 2 in the spatial dimension, giving us final data cubes, $150^2 \times 16$ in size. The final spatial pixel size is $0''.432 \times 0''.432$ (slightly less than an ACIS $0''.492$ pixel). We smoothed these data cubes with the non-local PCA method of Salmon et al. (2014). This method combines elements of dictionary learning and sparse patch-based representation of images (or spectral data cubes) for photon-limited data. Because this Poisson-PCA method is computationally intensive, relatively small ($150^2 \times 16$) data cubes, heavily binned along the spectral dimension as described above, were smoothed using patches $5^2 \times 6$ in size. The moderate spatial patch size of $2''.16 \times 2''.16$ preserves sharp spatial structures seen in the bright jets and in much fainter filamentary features found along the periphery of the PWN, while a large patch size in the spectral dimension is suitable for the synchrotron-

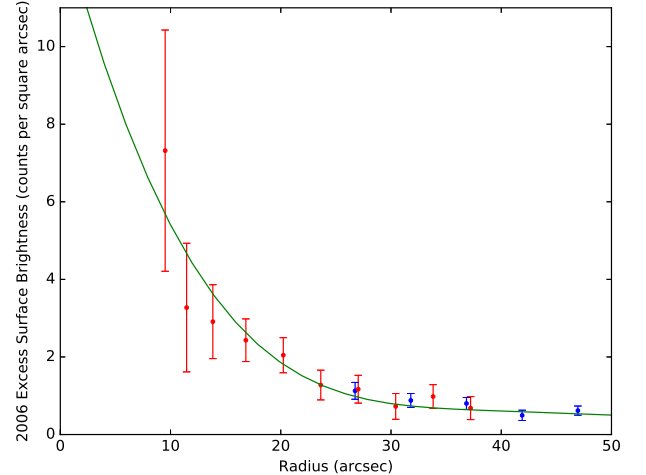


Figure 2. Radial profile of the 2006 X-ray halo at distances $< 50''$ away from the pulsar, for northern (in blue) and southeastern (in red) regions shown in Figure 1. Smoothed profile is in green.

dominated spectra of the PWN that vary smoothly across the entire spectral range of *Chandra*. With the patch size chosen, the most important parameters that control the smoothing of data cubes are the order l of the Poisson-PCA method, and the number of clusters K into which patches are grouped prior to estimation of intensities. We used $l = 6$ and $K = 30$ for the 2006 and 2016 data cubes of the Kes 75 PWN.

Images extracted from the smoothed data cubes must be corrected for effects of the time-varying background. We account for the time-varying particle background by determining the combined X-ray and particle background in a source-free region on the ACIS S3 chip, and then subtracting it from the smoothed images. However, the spatially-varying X-ray halo seen in the 2006 image (top panel in Figure 1) contributes most to the temporal background variations in the vicinity of the PWN. Within each of the concentric regions shown in the lower panel of Figure 1, we determined this halo contribution by subtracting the (exposure-weighted) 2016 image from the 2006 image. All these regions are centered on the pulsar. They are located outside of the PWN, including the innermost region only $10''$ southeast of the pulsar. If possible, they have been chosen not to overlap with the SNR shell emission seen in projection toward the center of the remnant. The measured radial surface brightness profile of the halo at distances $< 50''$ away from the pulsar is shown in Figure 2. A smoothed profile is also shown. The halo surface brightness north and southeast of the pulsar is well matched where they overlap in radius, fully consistent with a spherically-symmetric halo centered on the pulsar. Its brightness steeply increases toward the pulsar, suggesting that scattering of X-rays by the interstellar dust located between us and the pulsar is responsible for this transient halo. We use the smoothed profile shown in Figure 2 to model the halo contribution to the background at Epoch II. Since it is

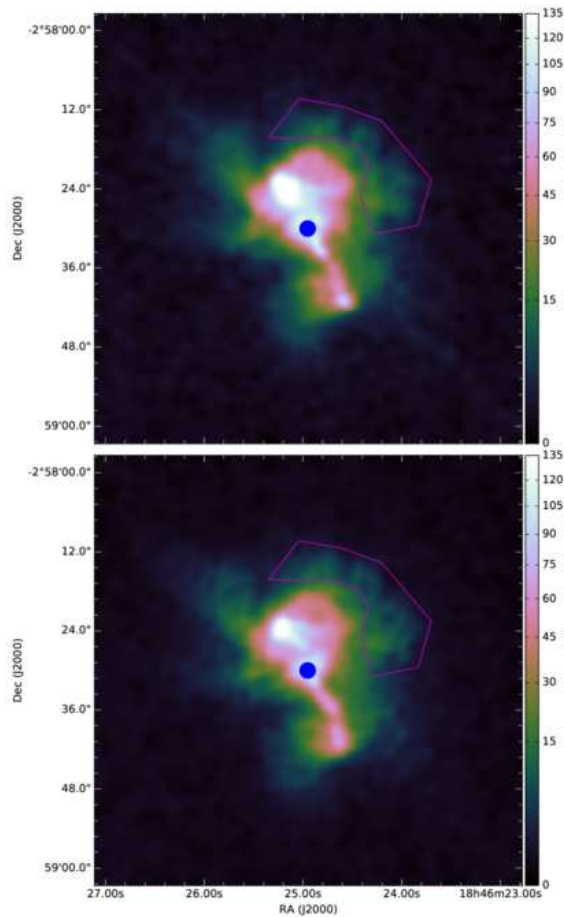


Figure 3. X-ray images of Kes 75 PWN in the 0.7–8 keV energy range from 2006 (top) and 2016 (bottom), smoothed with the non-local PCA method of Salmon et al. (2014). Background has been subtracted as described in the text. The pulsar has been masked out. Expansion of the PWN was measured along its northwest edge (within the region shown in magenta). Intensities are shown with the cubehelix color scheme of Green (2011). The scale is in counts per $0''.432 \times 0''.432$ image pixel.

difficult to measure the halo surface brightness profile close to the pulsar, this contribution must be considered as very uncertain at small ($< 10''$) distances away from the pulsar.

Images of the PWN extracted from the smoothed 2006 and 2016 data cubes, after background subtraction (including the halo contribution discussed above), are shown in Figure 3. These images, after normalization by monochromatic ($E = 3$ keV) exposure maps, are used as models for the complex spatial brightness distribution of the PWN. These models are fit to data consisting of unsmoothed images using the maximum likelihood method of Cash (1979) as appropriate for data dominated by Poisson statistics. In these fits, we allow for change in the physical image scale and in the surface brightness scale factor S . Expansion is centered on the pulsar. Except for Epoch II, a uniform background is assumed, with its value determined in a source-free region on

the ACIS S3 chip. For Epoch II, we add the X-ray halo to the background model, using the smoothed halo profile shown in Figure 2. Spatial variations in the effective exposure time are accounted for with help of the monochromatic ($E = 3$ keV) exposure maps.

The PWN is dominated by the prominent northern and southern jets whose morphologies have changed greatly between 2006 and 2016 (Figure 3). Near these jets, it is difficult to separate relatively slow motions expected from the PWN expansion from much more pronounced rapid changes caused by the short-term pulsar activity. Expansion of the PWN should be most easily detected far away from the jets where fast morphological and brightness variations are not expected. The relatively faint northwest rim of the PWN (see Figure 3) is the most suitable region for measuring expansion of the PWN as it occupies a substantial (over 90°) range in azimuth, and its irregular edge is relatively sharp.

We first measured expansion of the northwest rim of the PWN between Epochs II and IV using two image pairs: (1) smoothed 2016 and unsmoothed 2006 images, and (2) smoothed 2006 and unsmoothed 2016 images. Results are listed in the third and fourth rows of Table 2. The measured expansion is $2.38\% \pm 0.33\%$ and $2.17\% \pm 0.38\%$, respectively. Since these measurements are not independent, the small (0.2%) difference between them is caused by a bias inherent in our expansion measurement method. We attribute this systematic effect to smoothing that artificially makes the PWN slightly larger, leading to an overestimation of expansion for the image pair (1) and its underestimation for the image pair (2). Since exposure times are comparable for Epochs II and IV, this bias can be removed by averaging the measured expansions. The bias magnitude is 0.11% for each image pair, with the bias positive for the image pair (1) and negative for the image pair (2). The averaged expansion is $2.27\% \pm 0.51\%$ (errors have been added in quadrature to account for uncertainties in the smoothed images arising from photon noise). With the time baseline of 10 years, this corresponds to an expansion rate of $0.227\% \pm 0.051\% \text{ yr}^{-1}$.

The long (15.65 years) time baseline between Epochs I and IV allows for an independent and reliable measurement of expansion of the PWN northwest rim, although the short (32 ks) exposure time at Epoch I limits its accuracy. We used the smoothed 2016 image in combination with an unsmoothed 2000 image to arrive at an expansion of $4.27\% \pm 0.61\%$ (see the first row of Table 2). After reduction by 0.11% due to the bias caused by smoothing, the expansion becomes $4.16\% \pm 0.72\%$ (the error increased modestly as we combined in quadrature the statistical errors arising from photon noise for both epochs). This unbiased expansion measurement is listed in the second row of Table 2. The corresponding expansion rate, also listed in this Table, is $0.266\% \pm 0.046\% \text{ yr}^{-1}$, in good agreement with the expansion rate of $0.227\% \pm 0.051\% \text{ yr}^{-1}$ measured between Epochs II and IV.

We also measured expansion between Epochs III and IV in the same way as for Epochs I and IV (results are also listed in Table 2). The unbiased expansion rate is $0.249\% \pm 0.097\%$

Table 2. Expansion of Kes 75 Pulsar Wind Nebula

Baseline	Δt^a (year)	S^b	Expansion ^c (%)	Expansion Rate ^c (% yr ⁻¹)
2000 – 2016	15.65	1.222 ± 0.047	(4.27 ± 0.61)	(0.273 ± 0.039)
	15.65	...	4.16 ± 0.72	0.266 ± 0.046
2006 – 2016	10.00	1.148 ± 0.022	(2.38 ± 0.33)	(0.238 ± 0.033)
	10.00	$(0.857 \pm 0.017)^d$	$(2.17 \pm 0.38)^d$	$(0.216 \pm 0.038)^d$
	10.00	...	2.27 ± 0.51	0.227 ± 0.051
2009 – 2016	6.83	1.134 ± 0.037	(1.81 ± 0.54)	(0.265 ± 0.079)
	6.83	...	1.70 ± 0.66	0.249 ± 0.097
(2000+2006+2009) – 2016	0.249 ± 0.023

NOTE—Measurements were obtained in the region shown in Figure 3. All errors are 1σ . For each time baseline, the different lines differ in whether systematic effects were taken into account; values in parentheses are before correction for systematic effects.

^aBaseline length.

^bModel surface brightness scaling.

^cValues in brackets are before correction for systematic effects.

^dModel derived from the 2006 (instead of 2016) data.

yr⁻¹. The best estimate of the expansion rate, $0.249\% \pm 0.023\% \text{ yr}^{-1}$, is obtained by combining all three independent expansion rate measurements. The variance of these measurements is small, as reflected by the small error of $0.023\% \text{ yr}^{-1}$ for this averaged rate.

If the expansion is spatially uniform within the region shown in Figure 3 within which expansion is measured, the corresponding spatial velocity is proportional to distance from the pulsar. The irregular outer edge of the PWN in that region is at a radius of about $18''$, giving, for our adopted distance of 5.8 kpc, a velocity of 1200 km s^{-1} . Smaller radii then have proportionally smaller velocities. In Section 5 we adopt 1000 km s^{-1} as an estimate of the PWN expansion velocity.

There is a significant decrease in the surface brightness in 2016 for the PWN northwest rim (Table 2). When using the smoothed 2016 image as a model, the surface brightness scaling factor S varies between 1.13 and 1.22, systematically increasing with the measured expansion. In the absence of intrinsic flux variations, we expect S to be larger than unity, with $S - 1$ being twice as large as the measured expansion up to moderate (several percent) expansion values (Carlton et al. 2011). So we expect S to range from 1.04 for the Epoch III and IV image pair to 1.09 for the Epoch I and IV image pair. A decrease in flux of about 10% in 2016 is required to explain the larger than expected S obtained while fitting for expansion. For comparison, we estimate that the 2006 X-ray halo contribution to the measured flux of the PWN northwest rim

is only a few percent. So this flux decrease is highly significant and quite surprising.

4. FLUX AND MORPHOLOGY VARIATIONS

As was noted by Ng et al. (2008) and Livingstone et al. (2011), small-scale morphological changes occurred between 2000, 2006, and 2009. This has continued with the 2016 observations (Figure 4). The relative brightness of the northern knot (Figure 5) has varied significantly (see below), but there are no major changes. The ends of the jets appear not to move out significantly, though the southern jet end may move transversely slightly, and subtle outward motions of a feature just south of the pulsar were reported by Ng et al. (2008). Livingstone et al. (2011) show profiles along the jet, illustrating the relatively small changes from 2000 to 2009.

The X-ray bursts and glitch may have caused changes in the PWN flux, though neither Ng et al. (2008) nor Kumar & Safi-Harb (2008) found a significant change between 2000 and 2006. The pulsar was much brighter in 2006 than previously, by about a factor of 6 (Ng et al. 2008; Kumar & Safi-Harb 2008), contaminating the flux of the PWN with the trail of out-of-time events from the pulsar. More importantly, the excess scattered light we detect in the 2006 observation will contribute to the measured PWN flux. The model of Section 3, integrated over the region shown in Figure 1, accounts for about 5% of the total counts in the PWN for that epoch.

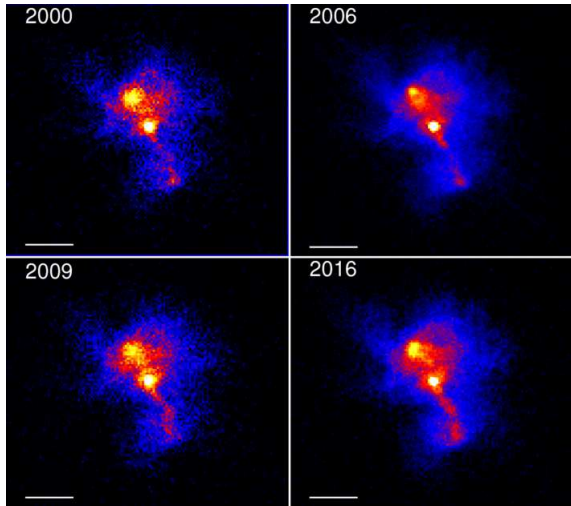


Figure 4. Images of the Kes 75 PWN at four epochs. No background has been subtracted. The white bar indicates $10''$.

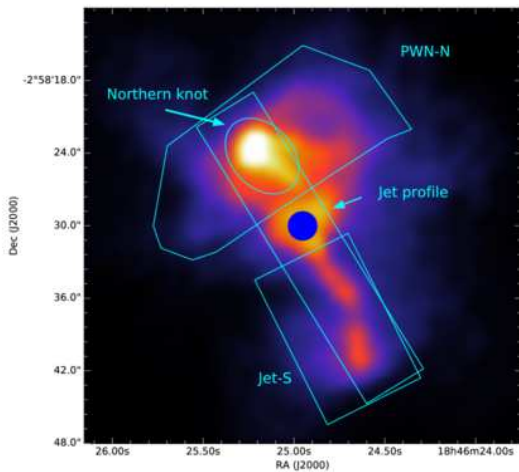


Figure 5. Regions used for subsequent analysis, superposed on smoothed 2016 image with pulsar removed. Long rectangle: region for jet profiles. Small ellipse: Northern knot. Northern cyan polygon: region PWN-N. Southern rectangle: region Jet-S.

The results of Section 3 indicate that the northwest rim of the PWN appears to have decreased in flux by about 10% between 2006 and 2016. Even taking into account a few percent excess flux in 2006 from the scattering halo, the decrease is significant and motivated a deeper investigation. To search for more extensive changes, we excluded a circular region $3''$ in diameter around the pulsar position from the region shown in the upper panel of Figure 1, and fit the PWN with a power-law with absorption, constraining the total (absorbed) flux rather than the normalization at some energy (XSPEC task `cfLUX`). This method gives absorbed fluxes that are relatively insensitive to the amount of absorption. To minimize

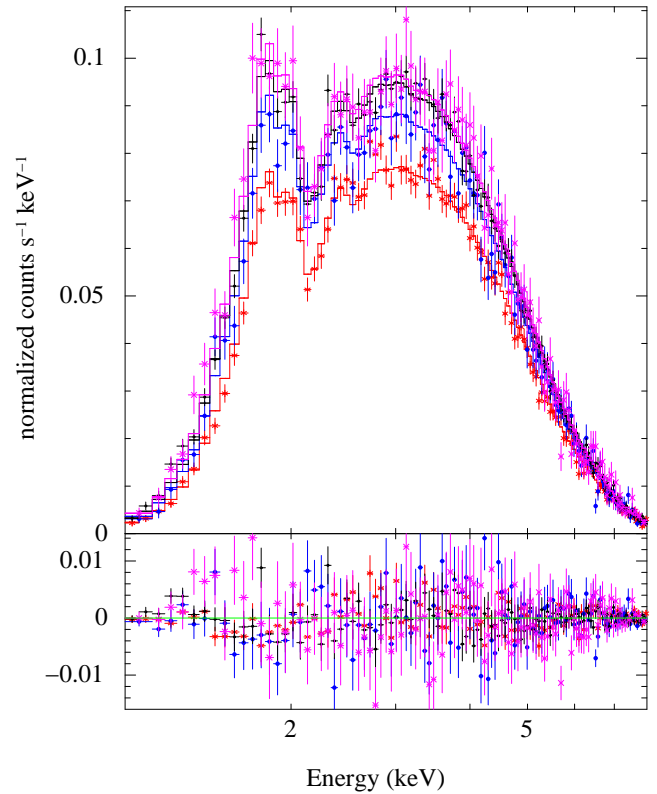


Figure 6. Spectra from four epochs for region PWN-N (the bulk of the northern nebula). From top down, data are from 2000, 2006, 2009, and 2016. Data have been binned by a factor of four, then adaptively binned, for display only. The models shown were fit as described in the text. The decrease with time is obvious.

effects of uncertainties in absorption, however, we fit spectra from all four epochs jointly, with absorbing column densities tied together. A similar method was used to measure fluxes in the three smaller regions shown in Figure 5. Figure 6 shows the spectra from all four epochs for region PWN-N, along with the model fits. The flux decrease is apparent. The results for integrated fluxes between 1 and 8 keV are shown in Table 3 and plotted in Figure 7. Errors given there are statistical only; systematic calibration errors can reach 3%². Thus changes above about 5% are significant.

We find that the PWN overall decreased in integrated flux between 2006 and 2016 by $(17 \pm 1)\%$, a highly significant change. If the 5% contribution in total counts in 2006 due to scattering produces a comparable contribution in total flux (i.e., neglecting differences in the spectrum of scattered pulsar X-rays and that of the PWN), the change is still of order 11%. In addition, the decrease from the 2000 value, $(12 \pm 2)\%$, is also significant, as is the decrease from 2009, $(9 \pm 2)\%$. However, the decrease is not spatially uniform. Jet profiles in Figure 8 show that the southern jet has remained roughly constant, while the northern one has expe-

² http://cxc.harvard.edu/cal/summary/Calibration_Status_Report.html#ACIS_EA

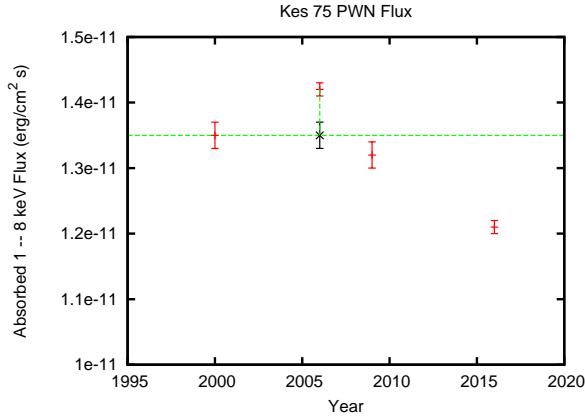


Figure 7. Total PWN flux, not corrected for absorption, excluding the pulsar (1 – 8 keV). The flux in 2006 is shown both before (red) and after (black) subtraction of the estimated scattering contribution. The horizontal line is the 2000 value.

rienced changes in morphology and overall brightness. Figure 9 quantifies this; the large northern portion of the PWN has faded by $(20 \pm 2)\%$ since 2000, with much of that decrease attributable to the bright northern knot which declined by $(30 \pm 4)\%$. The contribution of scattered light in the 2006 observation to total PWN flux is about 5% as mentioned above; in addition, scattered light contributes about 4% to region Jet-S, and about 1% to the northern knot. Figures 7 and 9 include the corrections to the total nebula and to region Jet-S.

The evidence for a flux decrease is unambiguous. However, we made an attempt to quantify its significance. The two short observations, in 2000 and 2009, provide the strictest test. First, we confront the well-known problem of using C statistics for estimates of goodness of fit (Connors & van Dyk 2007). Recent work (Kaastra 2017) provides some numerical approximations to allow the calculation of expectations C_e and variances $(\delta C)^2$ of the C statistic for particular situations. Our spectral fits for region PWN-N give values for $(C - C_e)/\delta C$ of -1.0 and 1.3 for the 2000 and 2009 fits – quite acceptable, and consistent with the visual impression of Figure 6.

We can provide a more rigorous test for the presence of the flux decrease using the likelihood-ratio test (LRT; Cash 1979). Our fitting indicates a drop in flux in Region PWN-N between 2000 and 2009 of 6.8%. To test the null hypothesis of no change in flux, we re-fit with the fluxes for those two years tied together. This produced an increase in the C statistic of 16.5. Using the LRT, we find that the likelihood of the null hypothesis is 4.7×10^{-5} . Other similar tests provide even more extreme rejections of the null hypothesis. However, since our statistical errors are no larger than the 3% systematic calibration errors, whose distribution is unknown, this exercise is of little quantitative value, and we have not performed it for other spectral fits.

Fitted photon indices Γ are shown in Table 4. When absorption values are fixed for all epochs, there are no signif-

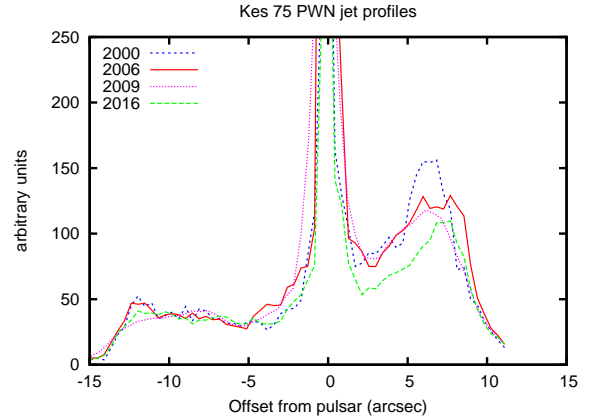


Figure 8. Profiles of the jet at four epochs, using region shown in Figure 5. Positive offsets are in the northern direction.

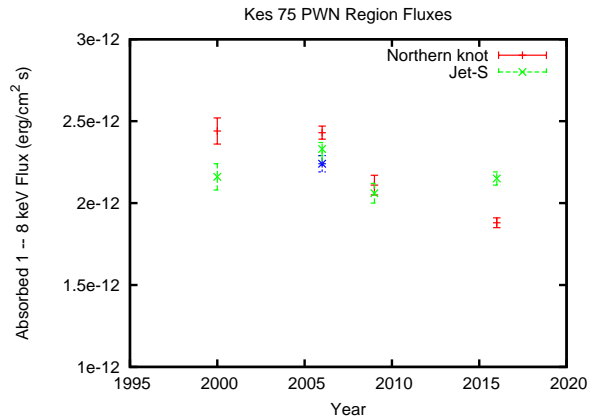


Figure 9. Fluxes of regions Jet-S (in green) and the northern knot (in red) (see Figure 5) as a function of time. The 2006 observation for Region Jet-S shows the flux corrected for scattered light (reduced by 4%); the 1% correction for the northern knot is within statistical measurement errors.

icant variations in photon index, even while the flux drops substantially by 2016 for all but the Jet-S region. The values we find tend to be steeper by about 0.1 than those reported in Ng et al. (2008), probably because our choice of Grevesse & Sauval (1998) abundances produces considerably larger absorbing column densities than those resulting from earlier abundance sets. However, we concur that the northern knot has a harder spectrum than the PWN as a whole.

5. DISCUSSION

5.1. PWN Expansion

The results of Table 2 give an expansion age $R/(dR/dt)$ of about 400 ± 40 years. If expansion had taken place at constant speed, this would be the true age. Since 2008, the pulsar has a period of 328 ms and a braking index n of 2.19 (Archibald et al. 2015), but before then, the braking index

Table 3. Kes 75 Pulsar-Wind Nebula Fluxes

Region	$F(2000)$	$F(2006)$	$F(2009)$	$F(2016)$
PWN ^a	13.5 ± 0.2	14.2 ± 0.1	13.2 ± 0.2	12.1 ± 0.1
PWN-N ^b	6.41 ± 0.13	6.42 ± 0.06	6.00 ± 0.11	5.34 ± 0.06
Northern knot ^c	2.44 ± 0.08	2.43 ± 0.04	2.11 ± 0.06	1.88 ± 0.03
Jet-S ^d	2.16 ± 0.08	2.33 ± 0.04	2.06 ± 0.06	2.15 ± 0.04

NOTE—Fluxes (1 – 8 keV) in units of 10^{-12} erg cm^{-2} s^{-1} , not corrected for absorption. Errors are 90% confidence.

$$^a N_H = 4.51 \pm 0.04 \times 10^{22} \text{ cm}^{-2}.$$

$$^b N_H = 4.48 \pm 0.06 \times 10^{22} \text{ cm}^{-2}.$$

$$^c N_H = 4.46 \pm 0.10 \times 10^{22} \text{ cm}^{-2}.$$

$$^d N_H = 4.71 \pm 0.11 \times 10^{22} \text{ cm}^{-2}.$$

Table 4. Kes 75 Pulsar-Wind Nebula Photon Indices

Region	$\Gamma(2000)$	$\Gamma(2006)$	$\Gamma(2009)$	$\Gamma(2016)$
PWN ^a	2.01 ± 0.03	2.03 ± 0.02	1.97 ± 0.03	2.00 ± 0.02
PWN-N ^b	1.99 ± 0.05	1.97 ± 0.03	1.94 ± 0.04	1.95 ± 0.03
Northern knot ^c	1.83 ± 0.08	1.81 ± 0.05	1.82 ± 0.07	1.83 ± 0.05
Jet-S ^d	1.89 ± 0.08	1.93 ± 0.05	1.97 ± 0.08	1.95 ± 0.05

NOTE—Fits are from 1 to 8 keV. Errors are 90% confidence.

$$^a N_H = 4.51 \pm 0.04 \times 10^{22} \text{ cm}^{-2}.$$

$$^b N_H = 4.48 \pm 0.06 \times 10^{22} \text{ cm}^{-2}.$$

$$^c N_H = 4.46 \pm 0.10 \times 10^{22} \text{ cm}^{-2}.$$

$$^d N_H = 4.71 \pm 0.11 \times 10^{22} \text{ cm}^{-2}.$$

was 2.65 (Livingstone et al. 2006). The dominant evolution of Kes 75 and its pulsar has taken place with the earlier value, which with due caution we take to have been constant since birth. For J1846–0258, the earlier value of n gives a decay index p (Equation 1) of 2.21.

For $t \lesssim \tau$, simple models (RC84; van der Swaluw et al. 2001) predict the PWN radius to grow as $R^{6/5}$, or an expansion index $m \equiv vt/R = 1.2$, so that the true age is 1.2 times the expansion age, or about 430 – 530 years. However, this gives $\tau \sim 350 - 450$ years, respectively, and (from Equation 1) L between 0.13 and 0.23 times L_0 . In this case, we might expect the expansion’s acceleration to have decreased toward $m = 1$, i.e., the calculation is not self-consistent. However, taking $m = 1$ similarly gives $L = (0.2 - 0.3)L_0$, close enough to L_0 that less deceleration will have occurred.

We conclude in any case that to within 50%, $t \sim \tau$, so we confirm that the true age of Kes 75 and its pulsar is between 360 and 530 years – the youngest known PWN in the Galaxy.

We performed our expansion measurement aligning the images on the pulsar itself. Even if the pulsar is moving with respect to the inner unshocked SN ejecta, those ejecta are expanding with a “Hubble law” velocity profile, $v \propto r$, and an observer at any location sees the same law. So the rate of expansion of the PWN with respect to the pulsar is unchanged. The question of a pulsar kick is an interesting one, though unrelated to our present concerns with the expansion and flux changes, but our data are not sufficient to determine the pulsar motion at this time.

The new smaller braking index of 2.19 produces a spin-down age of 1230 years and a larger value of p , 2.68, giving a more rapid dropoff of L with time, but also a larger $\tau = t_{\text{sd}} - t$. Again estimating with $m = 1.2$ for true ages of 430 – 530 years, we find $L = (0.2 - 0.3)L_0$, not inconsistent with the results for the earlier braking index. So the pulsar’s change in n does not make a large difference in the estimated age of the system. For a true age of 360 – 530 years and n of 2.19 or 2.65, the range of initial periods $P_0 = P(L/L_0)^{1/n+1}$ is 200 – 230 ms, and the initial luminosity in the range $(2.5 - 7.7)L = (2 - 6) \times 10^{37}$ erg s^{-1} . These conclusions are in line with previous studies (Bucciantini et al. 2011; Gelfand et al. 2014).

Our expansion rate corresponds to a current velocity of about 1000 km s^{-1} , for a distance of 5.8 kpc. A spherical bubble inflated by a constant-luminosity pulsar inside expanding uniform ejecta has after a time t a radius of

$$R = \left(\frac{125 v_1^3 L_0}{99 M_c} \right)^{1/5} t^{6/5} \quad (2)$$

where the total ejecta mass is M_c with outermost expansion velocity v_1 (Chevalier 1977; RC84). This can be rewritten in terms of the upstream ejecta density at time t , $\rho_{\text{ej}}(t) \propto t^{-3}$:

$$R = 0.79 L_0^{1/5} \rho_{\text{ej}}^{-1/5} t^{3/5}. \quad (3)$$

For $t = 480$ years, $R = 0.42$ pc, and assuming an intermediate value for the initial luminosity, $L_0 \sim 4 \times 10^{37}$ erg s^{-1} , we obtain a current upstream density $\rho_{\text{ej}} \sim 10^{-23}$ g cm^{-3} , and a swept-up mass of about $0.05 M_\odot$. That is, very little of the ejecta mass has been swept up. This rough estimate is consistent with the determination of a low total ejecta mass ($\sim 3 M_\odot$) of Gelfand et al. (2014), based on a similar model. However, in contrast to that work, we do not require any assumptions about the pulsar behavior other than that the luminosity has not changed radically since birth.

However, the assumption of uniform ejecta is clearly a gross oversimplification. While our result of a relatively low density currently being encountered by the PWN is robust, based only on the expansion velocity we measure and the pulsar’s luminosity, we cannot reliably infer a low total ejecta mass. In particular, the nickel bubble effect (Li et al. 1993) in which energy input from radioactive decay of ^{56}Ni in the

inner ejecta heats those ejecta, inflating a low-density bubble, could reduce the density of the inner ejecta. Chevalier (2005) considers this effect in the context of PWNe, and finds that for an initial red supergiant progenitor ejecta profile, the density contrast between the bubble material and ambient gas is given by

$$\frac{\rho_{\text{bub}} t^3}{\rho_{\text{amb}} t^3} = 0.052 \left(\frac{M_{\text{Ni}}}{0.1 M_{\odot}} \right)^{2/5} \left(\frac{\rho_{\text{amb}} t^3}{10^9 \text{ g s}^3 \text{ cm}^{-3}} \right)^{-2/5}. \quad (4)$$

That is, ejecta beyond the bubble could have more than an order of magnitude higher density and a much larger total mass. So a fairly ordinary supernova of type IIP, for which this is an appropriate normalization density, could produce a low-density bubble in which the PWN expands rapidly as observed.

In modeling the optical/IR spectrum of the Type IIP supernova SN 2004et, Jerkstrand et al. (2012) used a spherical hydrodynamic stellar model from Woosley & Heger (2007) but added artificial mixing in the core. The total density in their model was $\rho t^3 = 1.1 \times 10^9 \text{ g cm}^{-3} \text{ s}^3$, consistent with the ambient density in Chevalier’s picture. However, they deduced the presence of a nickel bubble with a filling factor of about 0.15 with mean density about $9 \times 10^{-16} t_{\text{yr}}^{-3} \text{ g cm}^{-3}$, which would give about $7 \times 10^{-24} \text{ g cm}^{-3}$ at an age of 480 years. They found that such a model satisfactorily describes the UVOIR spectra of SN 2004et between 140 and 700 days. The close agreement between the density of their nickel bubble and our inferred density from the simple PWN model is fortuitous, but the consistency of the two estimates supports the general idea of PWN expansion into a low-density nickel bubble in the interior of ejecta from a typical SN IIP event.

On the other hand, the idea of the origin of Kes 75 and its pulsar in a low-energy, low ejecta mass explosion may be problematic. Such explosions were discussed in Jerkstrand et al. (2015) in a study of Type IIB supernovae, using models with total ejecta masses below $3.5 M_{\odot}$, and core masses between 0.6 and $2.3 M_{\odot}$. Good descriptions of SN 1993J, SN 2008ax, and SN 2011dh were obtained from the lower end of this range, with mean core densities of $7 \times 10^6 \text{ g cm}^{-3} \text{ s}^3$ and $1 \times 10^7 \text{ g cm}^{-3} \text{ s}^3$ for core masses of 0.64 and $0.95 M_{\odot}$, respectively. However, only about $0.1 M_{\odot}$ of the ejecta mass was made up of ^{56}Ni , with a filling factor of 0.6 or larger, that is, a nickel bubble with a density lower by about an order of magnitude. At an age of 480 years, such a bubble would now have a density of a few times $10^{-25} \text{ g cm}^{-3}$, too low for our inferred density. While these models certainly do not exhaust the possibilities for low-mass core explosions, they suggest that such explanations for the Kes 75 event may be less likely than that of a normal SN IIP event.

It is instructive to compare the Kes 75 PWN with that of SNR B0540–693, inferred to have resulted from a Type IIP event. The exhaustive study of that object by Williams et al. (2008) showed that a similar model of accelerated PWN expansion in an iron-nickel bubble could explain observations at radio, IR, optical, and X-ray wavelengths. SNR

B0540–693 is about twice the age of Kes 75; in the picture of Williams et al. (2008) the age is 1140 years, and the PWN has expanded through the bubble and into the denser shell the bubble swept up in the first few years after the supernova. That dense shell has fragmented into mainly oxygen-rich clumps with a density contrast of about 100, with the PWN driving slow, radiative shocks into them. A simple spherically symmetric picture analogous to that of RC84 or Chevalier (2005) gave a current PWN shock velocity (i.e., excess of PWN bubble velocity over that of freely expanding ejecta) of about 150 km s^{-1} , and a mean density of $9 \times 10^{-24} \text{ g cm}^{-3}$ and total swept-up mass of about $1 M_{\odot}$. For Kes 75, we have a much smaller swept-up mass since the current nebular radius is about one-third that in SNR B0540–693, but a qualitatively similar picture can describe our observations. Though the extinction to Kes 75 is much too high for optical spectroscopy, IR emission from neutral oxygen at $63 \mu\text{m}$ has been reported from *Herschel* observations³, which we would attribute to shocked clumps as in SNR B0540–693. Clumping was invoked by Jerkstrand et al. (2012) and would be expected for the ejecta of a Type IIP supernova.

Given the asymmetry expected in SNe IIP events, and seen in young SNRs such as Cas A in which iron is highly asymmetrically distributed (e.g., Grefenstette et al. 2017), it is quite likely that a nickel bubble will not be centered on the expansion center. Such an off-center bubble makes an attractive explanation for the asymmetry in the PWN of Kes 75. It could produce considerably different ambient densities into which the two jets of the PWN are expanding (note that our expansion measurement would apply to the western edge of the northern half), as well as varying ejecta velocities and hence PWN shocks.

5.2. Flux Changes

Our finding of a flux increase of $(5 \pm 2)\%$ in the total PWN between 2000 and 2006 is marginally consistent with either the 3% reported by Ng et al. (2008) (based only on count rates) or the $(11_{-4}^{+3})\%$ value inferred by Kumar & Safi-Harb (2008). Even though our and their values are based on absorbed fluxes, the column density is so large ($N_{\text{H}} \sim 4 \times 10^{22} \text{ cm}^{-2}$) that changes in it can modify fitted fluxes by a few percent. Our choice of Grevesse & Sauval (1998) abundances gives very different fitted values for N_{H} (of order $4.6 \times 10^{22} \text{ cm}^{-2}$ instead of $4.0 \times 10^{22} \text{ cm}^{-2}$ as assumed by Ng et al.), so differences in fitted flux values of one or two percent are not unexpected between our results and those of Kumar & Safi-Harb (2008). However, comparison of our observed fluxes between epochs will not suffer from this cause.

Removing the 5% contribution to the 2006 PWN flux from scattered pulsar X-rays would reduce our inferred PWN flux to the same within errors as the flux from 2000, and supports our conclusion that the PWN itself has not brightened significantly in 2006. In addition, the 2009 flux is consistent with

³ Temim, T. 2016, in *Supernova Remnants: An Odyssey in Space after Stellar Death*, id. 50, <http://snr2016.astro.noa.gr>.

that from 2000. But the drop from 2009 to 2016 of $(9 \pm 2)\%$ is highly significant, and unprecedented in X-ray studies of pulsar-wind nebulae. We stress again that these statistical errors are always smaller than the systematic calibration errors of 3%, but that our results remain highly significant.

The flux decrease seems to occur over essentially the entire northern half of the PWN. From 2009 to 2016, the decrease in that region (PWN-N in Figure 5) is $(12 \pm 2)\%$ or about $1.8\% \text{ yr}^{-1}$. A spherical nebula, powered by a more-or-less isotropic injection of pulsar energy at a wind termination shock, can brighten on a timescale of the sound-crossing time of the nebula $\sqrt{3}R/c$ (assuming that the nebula is dominated by relativistic fluid with $\gamma = 4/3$ and sound speed $c/\sqrt{3}$), if the pulsar energy input somehow increases abruptly. However, the timescale for fading in this one-zone picture is simply the timescale for energy loss by adiabatic expansion or radiation; even if the pulsar suddenly ceased its energy injection, the bubble would fade only on a dynamical timescale (comparable to its age) or a synchrotron-loss timescale. Abrupt lowering of the magnetic field, due to causes unknown, could reduce the synchrotron flux, but would require the magnetic energy to be dissipated somehow without producing any additional radiation or other observable effect.

A more quantitative estimate of the evolutionary timescale is possible, including the continuing pulsar energy input. The age of the Kes 75 system t is about the same as the initial spindown timescale τ . Since the PWN is still encountering unshocked ejecta, the results of RC84 apply. There it is shown that for the part of the spectrum subject to synchrotron losses (true in the X-ray unless the magnetic-field strength is extremely weak), the spectral luminosity L_x decreases as $L_x \propto t^l$ with the index l related to the rate of magnetic-field decrease in the bubble, $B \propto t^{-b}$, to the injected spectral index of the initial particle distribution s ($N(E) = KE^{-s}$), and to the pulsar slowdown index p defined above. The relation is

$$L_x \propto t^l \text{ where } l = b \left(\frac{2-s}{2} \right) - p. \quad (5)$$

The X-ray photon index of the PWN near the pulsar is about $\Gamma \sim 1.6$, or an energy index $\alpha_x \sim 0.6$ (Ng et al. 2008). We expect a steepening due to losses of (approximately; see Reynolds 2009) 0.5 implying an injection (radio) value $\alpha_r \sim 0.1$ or $s = 2\alpha + 1 \sim 1.2$. (This is consistent with the somewhat uncertain radio spectrum; Bock & Gaensler 2005). If the magnetic energy evolved only by pulsar input and adiabatic expansion, $b = 1.3$ at this evolutionary stage (RC84); magnetic dissipation by reconnection or wave damping would cause B to decline faster, i.e., $b \geq 1.3$. For $b = 1.3$, $s = 1.2$, and using the pre-flare value $p = 2.21$, we find $l = -1.69$. This rate of decline implies a drop of 4% in 10 years, too slow to explain our observation. Using the post-flare value $p = 2.68$ gives $l = -2.16$ or a decline of 5%. While this estimate is rough, it does indicate that the gradual evolutionary changes expected for a young PWN cannot account for our observations. In any case, the absence

of significant decline between 2000 and 2006 argues strongly against any such gradual explanation.

Can radiative losses be responsible for the flux decrease? The synchrotron loss timescale ($t_{1/2}$, the time for an electron primarily radiating at frequency ν to lose half its energy) is given by

$$t_{1/2} = 1.2 \times 10^3 \left(\frac{h\nu}{1 \text{ keV}} \right)^{-1/2} \left(\frac{B}{10 \mu\text{G}} \right)^{-3/2} \text{ years.} \quad (6)$$

Terrier et al. (2008) estimate a magnetic-field strength of about $15 \mu\text{G}$, based on a simple scaling of the TeV to X-ray luminosity and the assumption that the TeV gamma-rays result from inverse-Compton upscattering cosmic microwave background photons by relativistic electrons (ICMB). However, the TeV spectrum is considerably softer than that in X-rays ($\Gamma \sim 2.3$; McBride et al. 2008), requiring intrinsic structure (i.e., not due to radiative losses) in the electron spectrum, as well as other assumptions. Such a low magnetic field in an object this young is unexpected; while there is no obvious physical reason to expect equipartition to be maintained between particles and magnetic field, the equipartition field for the Kes 75 PWN (based on the X-ray flux alone) is about $40 \mu\text{G}$ (Ng et al. 2008), while the field strength required to produce a bend in an originally unbroken particle spectrum at a frequency of order 10^{15} Hz (Morton et al. 2007) would be of order $100 \mu\text{G}$. For $B = 15 \mu\text{G}$, the loss time for electrons predominantly radiating at 5 keV is $t_{1/2} \sim 290$ years. Demanding $t_{1/2} \sim 10$ years implies $B \sim 140 \mu\text{G}$. Since the decline we observe began only in 2006 at the earliest, this value of B would have had to be reached fairly quickly, throughout the northern (but not southern) half of the nebula. This seems unreasonable. For no decline to be observed prior to 2006, we require $t_{1/2}$ before then to be greater than 6 years or $B \lesssim 100 \mu\text{G}$. If this value characterizes the northern half of the PWN, for a mean radius of $\sim 15''$ or $1.3 \times 10^{18} d_{5.8} \text{ cm}$, the magnetic energy content would be $U_B \sim 2 \times 10^{45} \text{ erg}$. The maximum pulsar input in 500 years, $L_0 t \sim (3-8)L(t)t$, is about $(0.4-1) \times 10^{48} \text{ erg}$ – certainly ample to provide this pre-flare field. However, then increasing B to $140 \mu\text{G}$ in only 10 years would require an additional $\Delta U_B \sim 2 \times 10^{45} \text{ erg}$, while at the current rate (unchanged by the flaring) the pulsar in 10 years injects only about this much energy. Even if these problems were overcome, the constancy of the photon index is not what would be expected in the event of suddenly increased radiative losses. Finally, such a picture would require the radio nebula to brighten substantially. The synchrotron luminosity depends on magnetic field as $B^{1+\alpha_r}$ or about $B^{1.2}$, so a flux increase by factor of at least $1.4^{1.2}$ or 50% would be expected, and could hardly be missed.

We are left with explanations relying on the inhomogeneity and anisotropy of the PWN – that is, on large departures from one-zone models. To reach the full extent of the northern nebula in 10 years requires a signal speed $v \gtrsim 0.14c$, considerably greater than the $0.03c$ inferred by Ng et al. (2008) for a small feature in the southern jet. Furthermore, the signal would need to be a decrease rather than increase in energy

input, even though substantial excess energy was released in the 2006 flares. More seriously, no change in spindown luminosity of the pulsar seems to have occurred (Archibald et al. 2015).

The distinct character of the northern and southern parts of the PWN has been noted before. Though they could not resolve substructures such as knots and jets, Bock & Gaensler (2005) pointed out that the two parts had different properties at mm wavelengths, with the northern part having a flatter spectrum (fainter than the south at 1.4 GHz but brighter at 86 GHz). They suggest additional spectral structure in the north as well. In the jet-torus model of Ng et al. (2008), the southern jet is approaching, making an angle of 28° with the plane of the sky. However, the brightest part of the jet is the northern knot, on the receding side. Bock & Gaensler (2005) attribute the southern emission to shell emission seen in projection, though the X-ray images do not seem consistent with this interpretation. As mentioned above, an iron-nickel bubble displaced from the pulsar could explain this asymmetry.

6. CONCLUSIONS

We have detected expansion in the PWN of the composite SNR Kes 75. Our measured PWN expansion of $(2.49 \pm 0.23)\%$ in 10 years gives free expansion ages of 400 ± 40 years. Theoretical expectations that the pulsar luminosity is still close to its birth value, and that the PWN is encountering roughly uniform ejecta, imply acceleration of the PWN with $R \propto t^{6/5}$, for which the true system age is larger by 1.2, or 480 years. We confirm directly, without recourse to inferences based on pulsar spindown models, that Kes 75 contains the youngest known pulsar-wind nebula in the Galaxy.

Our expansion rate implies a current expansion velocity of about 1000 km s^{-1} for the PWN. This relatively high velocity requires a rather low density for the material into which the PWN is expanding. While a low-energy supernova with small ejected mass cannot be ruled out, an attractive possibility is that the PWN is expanding into a low-density Fe-Ni bubble. If these elements were ejected anisotropically, the resulting asymmetric bubble could explain some of the symmetry between the two halves of the PWN.

As has been shown for the combination remnant B0540-693 in the LMC (Williams et al. 2008) and for the PWN G54.1+0.3 (Temim et al. 2010; Gelfand et al. 2015), the PWN in Kes 75 can probe inner supernova ejecta unobservable by other means, providing evidence on the nature of the progenitor system. Further observations of Kes 75, especially at infrared wavelengths, may allow firmer conclusions to be drawn, but what is currently known about Kes 75 seems consistent with an origin in a fairly typical Type IIP supernova. This finding, if confirmed, would add to the evidence that high magnetic-field neutron stars do not require unusual supernovae (e.g., Borkowski & Reynolds 2017).

The integrated 1 – 8 keV flux of the PWN has changed markedly since 2000. While an apparent rise in 2006 is likely due to scattered X-rays from the much brighter pulsar during its flaring seven days prior to the observations, we find a decline of over 10% in the total PWN flux between 2000 and 2016, mainly concentrated in the northern half of the PWN. A bright knot there has decreased in flux by $(30 \pm 4)\%$ since 2000. These changes are well in excess of typical calibration errors of order 3% and smaller statistical errors and are certainly real.

No good model exists for the fading. One-zone models do not easily accommodate such rapid changes, and are clearly oversimplified given the complex structure and inhomogeneity of the Kes 75 PWN. Properties requiring explanation include anisotropies in energy injection into the PWN (so the pulsar wind cannot be bilaterally symmetric), rapid changes in brightness occurring over a large volume, and absence of a significant change in the pulsar spindown luminosity to accompany the fading. The sudden change in braking index of PSR J1846–0258 in 2006 already pointed to difficulties with the simplest spindown inferences (Archibald et al. 2015), and our detection of major PWN changes without large changes to the pulsar spindown luminosity add to those difficulties. Kes 75 should continue to be monitored at X-ray and radio wavelengths, as it may contain clues demanding significant modifications to our ideas about pulsar winds and energy loss.

We acknowledge support from NASA through *Chandra* General Observer Program grant SAO GO6-17071X. PHG acknowledges support from NC State University’s Provost’s Professional Experience Program. We thank P. Plucinsky for discussions on systematic errors in flux calibration. The scientific results reported here are based on observations made by the *Chandra* X-ray Observatory. This research has made use of software provided by the *Chandra* X-ray Center (CXC) in the applications packages *CIAO* and *ChIPS*. We acknowledge use of various open-source software packages for Python, including Numpy, Scipy, Matplotlib, Astropy (a community-developed core Python package for Astronomy), and APLpy.⁴

Facilities: CXO

Software: CIAO (v 4.9) (Fruscione et al. 2006), XSPEC (Arnaud 1996), Astropy (The Astropy Collaboration et al. 2013), matplotlib (Hunter 2007), Numpy (van der Walt et al. 2011), Scipy⁵, APLpy (Robitaille & Bressert 2012)

⁴ APLpy is an open-source plotting package for Python hosted at <http://aplpy.github.com>.

⁵ Jones, E., Oliphant, T., Peterson, P., et al. 2001, <http://www.scipy.org>.

REFERENCES

- Akgün, T., Cerdá-Durán, P., Miralles, J. A., & Pons, J. A. 2017, *MNRAS*, 472, 3914
- Aller, H. D., & Reynolds, S. P. 1985, *ApJL*, 293, L73
- Antonopoulou, D., Espinoza, C. M., Kuiper, L., & Andersson, N. 2018, *MNRAS*, 473, 1644
- Archibald, A. M., Kaspi, V. M., Livingstone, M. A., & McLaughlin, M. A. 2008, *ApJ*, 688, 550
- Archibald, R. F., Kaspi, V. M., Beardmore, A. P., Gehrels, N., & Kennea, J. A. 2015, *ApJ*, 810, 67
- Arnaud, K. A. 1996, in *ASP Conf. Ser.*, Vol. 101, *Astronomical Data Analysis Software and Systems V*, ed. G. H. Jacoby & J. Barnes (San Francisco, CA: ASP), 17
- Becker, R. H., Helfand, D. J., & Szymkowiak, A. E. 1983, *ApJL*, 268, L93
- Becker, R. H., & Kundu, M. R. 1976, *ApJ*, 204, 427
- Bock, D. C.-J., & Gaensler, B. M. 2005, *ApJ*, 626, 343
- Borkowski, K. J., & Reynolds, S. P. 2017, *ApJ*, 846, 13
- Borkowski, K. J., Reynolds, S. P., Green, D. A., et al. 2014, *ApJL*, 790, L18
- Borkowski, K. J., Reynolds, S. P., & Roberts, M. S. E. 2016, *ApJ*, 819, 160
- Bucciantini, N., Arons, J., & Amato, E. 2011, *MNRAS*, 410, 381
- Carlton, A. K., Borkowski, K. J., Reynolds, S. P., et al. 2011, *ApJL*, 737, L22
- Cash, W. 1979, *ApJ*, 228, 939
- Chevalier, R. A. 1977, in *Astrophysics and Space Science Library*, Vol. 66, *Supernovae*, ed. D. N. Schramm (Berlin: Springer), 53
- Chevalier, R. A. 2005, *ApJ*, 619, 839
- Connors, A., & van Dyk, D. A. 2007, in *ASP Conf. Ser.*, Vol. 371, *Statistical Challenges in Modern Astronomy IV*, ed. G. J. Babu & E. D. Feigelson, 101
- Durant, M., Kargaltsev, O., Pavlov, G. G., Kropotina, J., & Levenfish, K. 2013, *ApJ*, 763, 72
- Espinoza, C. M., Lyne, A. G., & Stappers, B. W. 2017, *MNRAS*, 466, 147
- Fruscione, A., McDowell, J. C., Allen, G. E., et al. 2006, in *Proc.SPIE*, Vol. 6270, *Society of Photo-Optical Instrumentation Engineers (SPIE) Conference Series*, 62701V
- Gao, Z.-F., Wang, N., Shan, H., Li, X.-D., & Wang, W. 2017, *ApJ*, 849, 19
- Gavriil, F. P., Gonzalez, M. E., Gotthelf, E. V., et al. 2008, *Science*, 319, 1802
- Gelfand, J. D., Slane, P. O., & Temim, T. 2014, *AN*, 335, 318
—, 2015, *ApJ*, 807, 30
- Gelfand, J. D., Slane, P. O., & Zhang, W. 2009, *ApJ*, 703, 2051
- Gotthelf, E. V., Vasisht, G., Boylan-Kolchin, M., & Torii, K. 2000, *ApJL*, 542, L37
- Green, D. A. 2011, *BASI*, 39, 289
- Grefenstette, B. W., Fryer, C. L., Harrison, F. A., et al. 2017, *ApJ*, 834, 19
- Grevesse, N., & Sauval, A. J. 1998, *SSRv*, 85, 161
- Hester, J. J. 2008, *ARA&A*, 46, 127
- Hunter, J. D. 2007, *CSE*, 9.3, 90
- Jerkstrand, A., Ergon, M., Smartt, S. J., et al. 2015, *A&A*, 573, A12
- Jerkstrand, A., Fransson, C., Maguire, K., et al. 2012, *A&A*, 546, A28
- Kaastra, J. S. 2017, *A&A*, 605, A51
- Kaspi, V. M., Roberts, M. S. E., Vasisht, G., et al. 2001, *ApJ*, 560, 371
- Kim, M., Kim, D.-W., Wilkes, B. J., et al. 2007, *ApJS*, 169, 401
- Krishnamurthy, K., Raginsky, M., & Willett, R. 2010, *SIAM J. Imaging Sci.*, 3, 619
- Kumar, H. S., & Safi-Harb, S. 2008, *ApJL*, 678, L43
- Leahy, D. A., & Tian, W. W. 2008, *A&A*, 480, L25
- Li, H., McCray, R., & Sunyaev, R. A. 1993, *ApJ*, 419, 824
- Livingstone, M. A., Kaspi, V. M., Gotthelf, E. V., & Kuiper, L. 2006, *ApJ*, 647, 1286
- Livingstone, M. A., Ng, C.-Y., Kaspi, V. M., Gavriil, F. P., & Gotthelf, E. V. 2011, *ApJ*, 730, 66
- Lorimer, D. R., Faulkner, A. J., Lyne, A. G., et al. 2006, *MNRAS*, 372, 777
- McBride, V. A., Dean, A. J., Bazzano, A., et al. 2008, *A&A*, 477, 249
- Morton, T. D., Slane, P. O., Borkowski, K. J., et al. 2007, *ApJ*, 667, 219
- Ng, C.-Y., Slane, P. O., Gaensler, B. M., & Hughes, J. P. 2008, *ApJ*, 686, 508
- Reynolds, S. P. 2009, *ApJ*, 703, 662
- Reynolds, S. P., & Chevalier, R. A. 1984, *ApJ*, 278, 630
- Robitaille, T., & Bressert, E. 2012, *Astrophysics Source Code Library*, *APLpy: Astronomical Plotting Library in Python*, ascl:1208.017
- Salmon, J., Harmany, Z., Deledalle, C.-A., & Willett, R. 2014, *J.Math.Imaging Vis.*, 48, 279
- Temim, T., Slane, P., Reynolds, S. P., Raymond, J. C., & Borkowski, K. J. 2010, *ApJ*, 710, 309
- Terrier, R., Djannati-Atai, A., Hoppe, S., et al. 2008, in *AIP Conf. Ser.*, Vol. 1085, *4th Heidelberg International Symposium on High-Energy Gamma-Ray Astronomy*, ed. F. A. Aharonian, W. Hofmann, & F. Rieger (New York: AIP), 316
- The Astropy Collaboration, Robitaille, T. P., Tollerud, E. J., et al. 2013, *A&A*, 558, 33
- van der Swaluw, E., Achterberg, A., Gallant, Y. A., & Tóth, G. 2001, *A&A*, 380, 309
- van der Walt, S., Colbert, S. C., & Varoquaux, G. 2011, *CSE*, 13.2, 22

Verbiest, J. P. W., Weisberg, J. M., Chael, A. A., Lee, K. J., &
Lorimer, D. R. 2012, ApJ, 755, 39

Williams, B. J., Borkowski, K. J., Reynolds, S. P., et al. 2008, ApJ,
687, 1054

Woosley, S. E., & Heger, A. 2007, Phys.Rep., 442, 269